



ELSEVIER

SCIENCE @ DIRECT®

PHYSICS LETTERS B

Physics Letters B 608 (2005) 47–52

[www.elsevier.com/locate/physletb](http://www.elsevier.com/locate/physletb)

## Effect of kinematics on final state interactions in $(e, e'p)$ reactions

C. Barbieri <sup>a</sup>, D. Rohe <sup>b</sup>, I. Sick <sup>b</sup>, L. Lapikás <sup>c</sup>

<sup>a</sup> TRIUMF, 4004 Wesbrook Mall, Vancouver, British Columbia, Canada V6T 2A3  
<sup>b</sup> Departament für Physik und Astronomie, Universität Basel, CH-4056, Switzerland  
<sup>c</sup> NIKHEF, P.O. Box 41882, 1009 DB Amsterdam, The Netherlands

Received 16 November 2004; received in revised form 22 December 2004; accepted 27 December 2004

Available online 4 January 2005

Editor: W. Haxton

### Abstract

Recent data from experiment E97-006 at TJNAF using the  $^{12}\text{C}(e, e'p)$  reaction at very large missing energies and momenta are compared with a calculation of two-step rescattering. A comparison between parallel and perpendicular kinematics suggests that the effects of final state interactions can be strongly reduced in the former case.

© 2005 Elsevier B.V. All rights reserved.

PACS: 25.30.Fj; 25.30.Dh; 21.60.-n; 21.10.Pc; 21.10.Jx

Keywords: Electron scattering; Short-range correlations

Short-range and tensor correlations (SRC) have long been known to be one of the major elements influencing the dynamics of nuclear systems [1,2]. Their main effects consist in shifting a sizable amount of spectral strength, 10–20% [3], to very high energies and momenta. This results in an equally large depletion of quasi-particle orbitals [4], which is fairly independent of the given shell and the nuclear mass number. Several theoretical studies, based on realistic phenomenological  $NN$  interactions, have suggested that most of the correlated strength is found along

a ridge in the momentum–energy plane ( $k$ – $E$ ). This spans a region of several hundred MeV/ $c$  (MeV) [5–7] which corresponds to large missing momenta ( $p_m$ ) and energies ( $E_m$ ) in knock out cross sections. This contribution to the spectral function is also responsible for most of the binding energy of nuclear systems [8]. The main characteristics predicted by these calculations are consistent with recent experimental data [9,10], which will be considered further below.

An accurate experimental determination of the correlated strength in the hole spectral function  $S^h(p_m, E_m)$  would represent an important advance in our understanding of SRC, but locating this strength at both large  $E_m$  and  $p_m$  is difficult. Early attempts done by

E-mail address: [barbieri@triumf.ca](mailto:barbieri@triumf.ca) (C. Barbieri).

means of  $(e, e'p)$  reactions found an enormous background generated by final state interactions (FSI), see, for example, Refs. [11,12]. The principal reason is that the correlated strength is spread over an energy range of several hundred MeV, so the total density of the spectral function is very low. In this energy regime multi-nucleon processes, beyond the direct knock out, are possible [13] and can induce large shifts in the missing energies and momenta, moving strength to regions where the direct signal is much smaller and therefore submerges it. Calculations of FSI effects were done by several groups [13–17]. In general, theory predicts larger effects when the transverse structure functions that enter the expression of the  $(e, e'p)$  cross section dominate the longitudinal one. Interference effects between FSI and initial state correlations (IC) can also play a role [16]. The results of Refs. [14, 18] suggests that multiple rescattering contributions (more than two-steps) are relatively small in light nuclei and when parallel kinematics are considered.<sup>1</sup> However, it is clear that the identification of the correlated strength cannot be achieved unless the contributions from FSI can be reduced, by the choice of kinematics, to a size where they can be handled by calculations. This issue has been recently discussed in detail in Ref. [19]. It was already addressed in the proposal of experiment E97-006 [20] where a Monte Carlo simulation and kinematical arguments lead to the suggestion that the best chance for an identification of SRC occurs in parallel kinematics. The latter tend to be less sensitive to meson exchange currents (MEC)—which involve transverse excitations—and are cleaner due to the high momentum that is required for the detected proton. New data were subsequently taken by the E97-006 Collaboration at Jefferson Lab [9,10,21] for a set of nuclei ranging from carbon to gold. Both optimal (parallel) and perpendicular kinematics were used, to provide useful data for investigating the reaction mechanism.

In the energy regime of the JLab experiment, the relevant contribution to FSI is identified with two-

step rescattering. This has been studied recently in Ref. [22] using a semiclassical model. The particular approach taken there already has the advantage of describing the distortion due to FSI in terms of the full one hole spectral function. This takes into account both the momentum and energy distribution of the original correlated strength, which is of importance for the proper description of the response [23]. In this Letter we carry out a first comparison of the prediction of Ref. [22] with the data of Ref. [21] for the nucleus  $^{12}\text{C}$ .

We consider contributions to the experimental yield that come from two-step mechanisms in which the knock out reaction  $(e, e'a)$  for a nucleon  $a$  is followed by a scattering process from a nucleon in the medium,  $N'(a, p)N''$ , eventually leading to the emission of the detected proton and the undetected nucleon  $N''$ . Three channels are considered in the present work, in which  $a$  represents either a proton (with  $N' = p$  or  $n$ ) or a neutron (with  $N' = p$ ). The semi-exclusive cross section for these events was calculated according to Ref. [22] as

$$\begin{aligned} & \frac{d^6\sigma_{\text{rescatt}}}{dE_0 d\Omega_{\hat{k}_0} dE_f d\Omega_{\hat{p}_f}} \\ &= \sum_{a, N'=1,2,3} \int d\mathbf{r}_1 \int d\mathbf{r}_2 \int_0^\omega dT_a \\ & \times \rho_N(\mathbf{r}_1) \frac{K S_a^h(|\mathbf{q} - \mathbf{p}_a|, \omega - E_a) \sigma_{ea}^{cc}}{M(\mathbf{r}_1 - \mathbf{r}_2)^2} \\ & \times g_{aN'}(|\mathbf{r}_1 - \mathbf{r}_2|) P_T(p_a; \mathbf{r}_1, \mathbf{r}_2) \rho_{N'}(\mathbf{r}_2) \\ & \times \frac{d^3\sigma_{aN'}}{dE_f d\Omega_{\hat{p}_f}} P_T(p_f; \mathbf{r}_2, \infty), \end{aligned} \quad (1)$$

where  $(E_0, \mathbf{k}_0)$ ,  $(E_f, \mathbf{p}_f)$  and  $(\omega, \mathbf{q})$  represent the four-momenta of the detected electron, the final proton and the virtual photon, respectively. Eq. (1) assumes that the intermediate particle  $a$  is generated in plane wave impulse approximation (PWIA) by the electromagnetic current at a point  $\mathbf{r}_1$  inside the nucleus. Here  $K = |\mathbf{p}_a|E_a$  is a phase space factor,  $S_a^h(k, E)/M$  is the spectral function of the hit particle  $a$  normalized to one (i.e.,  $M = N(Z)$  if  $a$  is a neutron (proton)) and  $\sigma_{ea}^{cc}$  the electron–nucleon cross section. In the calculations below we used the  $\sigma^{cc}$  prescription discussed in Ref. [21], which is obtained by employing the on-shell

<sup>1</sup> In this work we refer to ‘parallel’ and ‘perpendicular’ kinematics in terms of the angle between the momentum transferred by the electron  $\mathbf{q}$  and the momentum of the initial nucleon  $\mathbf{p}_i = -\mathbf{p}_m$  (as opposed to the final proton  $\mathbf{p}_f$ ). This definition is more restrictive in the limit of high momentum transfer, where  $\mathbf{q}$  and  $\mathbf{p}_f$  tend to be collinear.

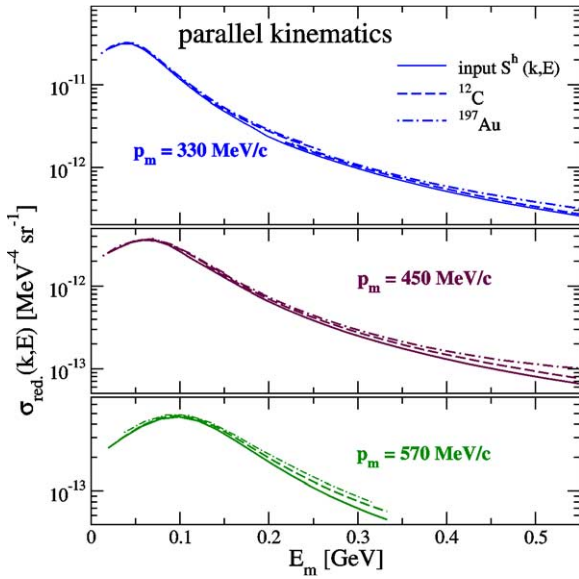


Fig. 1. (Color online.) Theoretical reduced cross section in the correlated region obtained in parallel kinematics for  $^{12}\text{C}$  (dashed-line) and  $^{197}\text{Au}$  (dot-dashed line) targets. The results for gold have been normalized to the number of protons in carbon, for comparison. The full line shows the model spectral function, Eq. (3).

current also for off-shell protons.<sup>2</sup> The pair distribution functions  $g_{aN'}(|\mathbf{r}_1 - \mathbf{r}_2|)$  account for the joint probability of finding a nucleon  $N'$  at  $\mathbf{r}_2$  after the particle  $a$  has been struck at  $\mathbf{r}_1$  [25]. The integration over the kinetic energy  $T_a$  of the intermediate nucleon  $a$  ranges from 0 to the energy  $\omega$  transferred by the electron. The point nucleon densities  $\rho_N(\mathbf{r})$  were derived from experimental charge distributions by unfolding the proton size [26] and the factor  $P_T(p; \mathbf{r}_1, \mathbf{r}_2)$  gives the transmission probability that the struck particle  $a$  propagates, without any interactions, to a second point  $\mathbf{r}_2$ , where it scatters from the nucleon  $N'$  with cross section  $d^3\sigma_{aN'}$ . The latter was obtained by adding the constraints of Pauli blocking to the vacuum nucleon–nucleon (NN) cross section and accounting for the Fermi distribution of the hit nucleon [22]. This ap-

<sup>2</sup> Preferably one uses a prescription to extrapolate the on-shell cross section to the off-shell case while preserving energy and current conservation. The analysis of several possible prescriptions carried out in Ref. [21] found that the best agreement between the data of different kinematics is obtained by avoiding any of the ad hoc modifications of the kinematics at the electromagnetic vertex as suggested in Ref. [24].

proach is accurate for the kinematics of this work since at large nucleon momenta the dispersion effects of the medium become negligible.

Fig. 1 shows the reduced cross section for both  $^{12}\text{C}$  and  $^{197}\text{Au}$  targets defined as  $\sigma_{\text{red}}(p_m, E_m) = (\sigma_{\text{PWIA}} + \sigma_{\text{rescatt}})/(|p_f E_f| \sigma_{ep}^{cc} T)$ , where  $\sigma_{\text{PWIA}}$  is the PWIA cross section of the direct process and  $T$  the nuclear transparency. For the case of gold, the results have been normalized according to the number of protons in  $^{12}\text{C}$ , for comparison. Eq. (1) predicts small contributions of FSI for parallel kinematics, with a slight increase at very large missing energies [22]. It is important to observe that the main reason for the small effects of rescattering obtained in this calculation is kinematical in origin. Due to rescattering events, the emitted nucleon loses part of its initial energy by knocking out a second particle. The requirement of small angles between the momenta  $\mathbf{q}$  and  $\mathbf{p}_i$  implies even larger energies  $T_a$  (i.e., small  $E_m$ ) and missing momenta for the intermediate nucleon. Therefore, the rescattered strength is sampled in regions where the correlated spectral function is smaller than for the direct process. For analogous reasons, multiple rescattering effects become even less important, as seen in Ref. [14] for perfectly parallel kinematics.

Recently, the experimental strength measured for  $^{12}\text{C}$  in parallel kinematics was compared to theory [9,10]. For missing energies up to 200 MeV, the summed strength measured turned out to agree with theoretical predictions. Also, the ridge-like shape of strength distribution was observed except that the position of the peak was found at lower missing energies than predicted by theory. This gives confidence that, for the first time, effects of the high momentum components attributed to SRC could be observed without being overwhelmed by the distortion of FSI. However, a quantitative understanding of the reaction mechanism is still needed.

In order to make a meaningful comparison between the experiment and the theoretical predictions for rescattering we need a proper ansatz for the undistorted spectral function,  $S^h(k, E)$  in Eq. (1). At low energies and momenta we employed the correlated part of the spectral function  $S_{\text{LDA}}^h(k, E)$  in Ref. [6], which was obtained using local density approximation (LDA), and combined it with a proper scaled spectral function  $S_{\text{WS}}^h(k, E)$  derived from a Wood–Saxon potential. The parameters of the Wood–Saxon potential

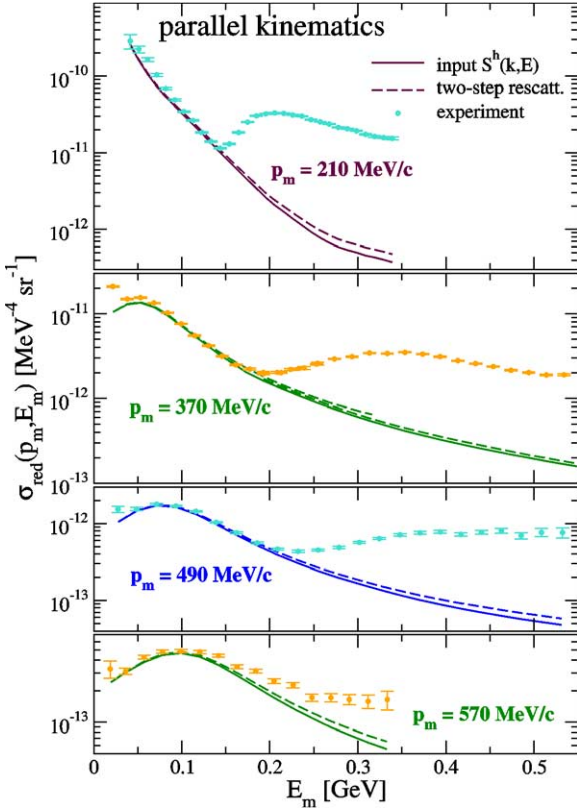


Fig. 2. Theoretical results for the reduced cross section of  $^{12}\text{C}$  obtained in parallel kinematics (dashed line) compared with the experimental results of Ref. [21]. The full line shows the model spectral function of Eq. (3) employed in the calculations.

were adjusted to previous data. This includes the bulk of the spectral strength, located in the mean field (MF) region up to a momentum of  $\approx 250$  MeV/c. However, the position of the SRC correlated peak at large momenta is not well reproduced by calculations [10]. The latter represents only a fraction of the total number of nucleons in the system but it is the part probed in the experiment under consideration. Given the above considerations regarding the results of Refs. [9,10], it is appropriate to extract the spectral function in the correlated region from the experimental data. We choose to employ  $S_{\text{LDA+WS}}^h(k, E)$  for the MF part but to substitute it in the SRC region with a parameterization in terms of a Lorentzian energy distribution

$$S_{\text{corr}}^h(k, E) = \frac{C e^{-\alpha k}}{[E - e(k)]^2 + [\Gamma(k)/2]^2}, \quad (2)$$

which was fitted to the experimental results for  $^{12}\text{C}$  in parallel kinematics. Linear functions of momentum  $e(k)$  and  $\Gamma(k)$  were sufficient to obtain a fit of the region around the top of the correlated ridge, where the experiment appears to be free from FSI effects. The shape assumed for the spectral function at very high energies is then determined by Eq. (2). The quality of the fit can be judged from Fig. 2. The full spectral function employed in Eq. (1) is

$$S^h(k, E) = \begin{cases} S_{\text{corr}}^h(k, E) & \text{for } k > 230 \text{ MeV}/c, E > 19 \text{ MeV}, \\ S_{\text{LDA+WS}}^h(k, E) & \text{otherwise.} \end{cases} \quad (3)$$

This choice provides a smooth transition between the mean-field and the correlated parts and gives well behaved distributions of energy and momentum, obtained by integrating  $S^h(k, E)$  over  $\mathbf{k}$  and  $E$ , respectively. The total number of protons predicted by Eq. (3) is 5.97. For  $^{12}\text{C}$  the same spectral function was employed for both protons and neutrons. For  $^{197}\text{Au}$  an analogous construction of  $S^h(k, E)$  was done, which used the same  $S_{\text{corr}}^h(k, E)$  of Eq. (2) normalized according to the correct number of protons or neutrons.

Fig. 2 compares the experimental data for parallel kinematics with the results of Eq. (1). The experiment agrees with parameterization, Eq. (2), at low missing energies. At larger energies the total experimental strength starts increasing again and becomes more than an order of magnitude larger than the direct signal. The fact that this deviation starts sharply at the pion production threshold,  $E_m \approx 150$  MeV, indicates that  $(e, e' p \pi)$  gives a large contribution. This reaction produces a distorted image of the correlated region at larger missing energies (due to the extra energy necessary for creating the pion). At even larger missing energies, other mesons can be produced and the experimental  $E_m$ -distribution becomes rather flat. As the missing momentum increases, the regions dominated by correlated nucleons and pion production tend to overlap. We note that as long as multiple rescattering effects can be neglected, quantum interference is not expected to play a role since these reaction mechanisms lead to different particles in their final states.

The experimental data are found to be sensibly larger in perpendicular kinematics than in parallel ones. The discrepancy between the two cases increases with the missing momentum and reaches one order of



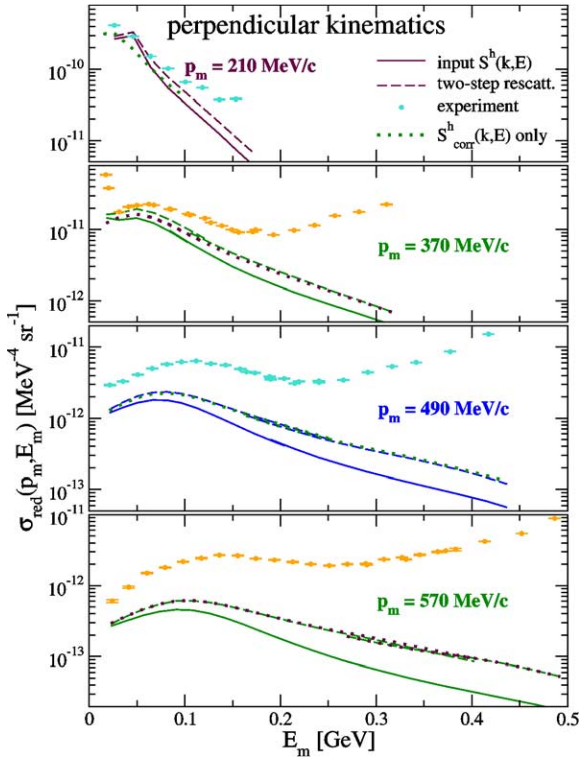


Fig. 3. Theoretical results for the reduced cross section of  $^{12}\text{C}$  obtained in perpendicular kinematics (dashed line) compared with the experimental results of Ref. [21]. The full line shows the model spectral function of Eq. (3) employed in the calculations. The dotted lines show the results obtained by neglecting the rescattering from the MF region,  $S_{\text{LDA+WS}}^h(k, E)$ , in Eq. (3). This becomes indistinguishable from the full calculation for  $p_m > 450$  MeV/c.

magnitude at very large  $p_m$ . Due to the much larger redistribution of spectral strength the valley between the SRC and meson production regions is also filled in and it is no longer possible to distinguish them. The data for perpendicular kinematics are compared with the results of Eq. (1) in Fig. 3. In this case, the rescattered strength is large and affects the reduced spectral function already at the top of the SRC tail. Kinematically, this can be understood by observing that for perpendicular kinematics a nucleon can lose energy in a rescattering event and still be detected with a missing momentum larger than its initial momentum. This results in moving strength from regions where the spectral function is large to regions where it is small, thereby submerging the direct signal. The shift is large enough that measurements in the cor-

related region can be affected by events originating from the MF orbits [22]. This is displayed by the dotted lines in Fig. 3, which have been obtained by setting  $S_{\text{LDA+WS}}^h(k, E) = 0$  in Eq. (3). The effect of neglecting rescattering from the MF strength is appreciable for missing momenta lower than 500 MeV/c, but becomes negligible above it. For parallel kinematics a similar comparison shows no visible effects indicating that rescattering moves strength *only* within the correlated region itself. Fig. 3 shows that the Eq. (1) can account for the differences between parallel and perpendicular kinematics for  $E_m \approx 50$  MeV and  $p_m < 350$  MeV/c. However, it strongly underpredicts the experiment over the larger part of the correlated region. For  $p_m = 600$  MeV/c, the cross section is predicted to be 50% larger than the direct process, whereas the experiment is about of one order of magnitude above. Moreover, the experimental data for perpendicular kinematics show a further rise for  $E_m \geq 200$  MeV, in the region of meson production. We conclude that two-step rescattering represents only a fraction of the total FSI present in perpendicular kinematics. A possible contribution that could bring theory and data closer together would be that of MEC currents that involve the excitation of a  $\Delta$  or higher resonances; these are known to be sensitive to transverse degrees of freedom. Besides, the effects of multiple rescattering and IC can become relevant, especially for heavy nuclei [15,16].

In conclusion, we have carried out a comparison of the experimental  $(e, e'p)$  data at large  $p_m - E_m$  with first theoretical predictions of rescattering effects for the same kinematics. The results are understood in terms of kinematical constraints and confirm the expectation that, for light nuclei and properly chosen parallel kinematics, the effects of FSI can be small for missing energies up to the  $\pi$  emission threshold. In perpendicular kinematics the agreement between data and theory is less favorable. This suggests that additional ingredients, of transverse character, such as MEC, should be included in the calculations.

## Acknowledgements

This work is supported by the Natural Sciences and Engineering Research Council of Canada (NSERC), by the Schweizerische Nationalfonds (NSF) and by

the “Stichting voor Fundamenteel Onderzoek der Materie (FOM)”, which is financially supported by the “Nederlandse Organisatie voor Wetenschappelijk Onderzoek (NWO)”.

## References

- [1] V.R. Pandharipande, I. Sick, P.K.A. deWitt Huberts, *Rev. Mod. Phys.* 69 (1997) 981.
- [2] W.H. Dickhoff, C. Barbieri, *Prog. Part. Nucl. Phys.* 52 (2004) 377.
- [3] B.E. Vonderfecht, W.H. Dickhoff, A. Polls, A. Ramos, *Phys. Rev. C* 44 (1991) R1265.
- [4] M.F. van Batenburg, Ph.D. Thesis, University of Utrecht, 2001.
- [5] C. Ciofi degli Atti, S. Liuti, S. Simula, *Phys. Rev. C* 41 (1990) R2474.
- [6] O. Benhar, A. Fabrocini, S. Fantoni, I. Sick, *Nucl. Phys. A* 579 (1994) 493.
- [7] H. Mütter, W.H. Dickhoff, *Phys. Rev. C* 49 (1994) R17; H. Mütter, W.H. Dickhoff, A. Polls, *Phys. Rev. C* 51 (1995) 3040.
- [8] Y. Dewulf, W.H. Dickhoff, D. Van Neck, E.R. Stoddard, M. Waroquier, *Phys. Rev. Lett.* 90 (2003) 152501.
- [9] D. Rohe, et al., *Phys. Rev. Lett.* 93 (2004) 182501.
- [10] T. Frick, Kh.S.A. Hassaneen, D. Rohe, H. Mütter, *Phys. Rev. C* 70 (2004) 024309.
- [11] R.W. Lourie, et al., *Phys. Rev. Lett.* 56 (1986) 2364.
- [12] H. Baghaei, et al., *Phys. Rev. C* 39 (1989) 177; L.B. Weinstein, et al., *Phys. Rev. Lett.* 64 (1990) 1646.
- [13] T. Takaki, *Phys. Rev. Lett.* 62 (1989) 395.
- [14] P. Demetriou, S. Boffi, C. Giusti, F.D. Pacati, *Nucl. Phys. A* 625 (1997) 513.
- [15] N.N. Nikolaev, et al., *Nucl. Phys. A* 582 (1995) 665.
- [16] A. Bianconi, S. Jeschonnek, N.N. Nikolaev, B.G. Zakharov, *Nucl. Phys. A* 608 (1996) 437; H. Morita, C. Ciofi degli Atti, T. Treleani, *Phys. Rev. C* 60 (1999) 034603.
- [17] S. Janssen, J. Ryckebusch, W. Van Nespren, D. Debruyne, *Nucl. Phys. A* 672 (2000) 285.
- [18] J. Ryckebusch, D. Debruyne, P. Lava, S. Janssen, B. Van Overmeire, T. Van Caueren, *Nucl. Phys. A* 728 (2003) 226.
- [19] I. Sick, in: O. Benhar, A. Fabrocini (Eds.), *Electron Nucleus Scattering*, World Scientific, Singapore, 1997, p. 445.
- [20] I. Sick, et al., *Jlab-Proposal E97-006* (1997).
- [21] D. Rohe, *Habilitationsschrift*, University of Basel, 2004 (unpublished).
- [22] C. Barbieri, L. Lapikás, *Phys. Rev. C* 70 (2004) 054612.
- [23] O. Benhar, A. Fabrocini, S. Fantoni, *Phys. Rev. Lett.* 87 (2001) 052501.
- [24] T. de Forest Jr., *Nucl. Phys. A* 392 (1983) 232.
- [25] R. Schiavilla, D.S. Lewart, V.R. Pandharipande, S.C. Pieper, R.B. Wiringa, S. Fantoni, *Nucl. Phys. A* 473 (1987) 267.
- [26] H. de Vries, C.W. de Jager, C. de Vries, *At. Data Nucl. Data Tables* 36 (1987) 495.